NIH Public Access
Author Manuscript
Cell Transplant. Author manuscript; available in PMC 2014 January 15.

Published in final edited form as:
Cell Transplant. 2013 ; 22(8): 1395–1408. doi:10.3727/096368912X653264.

Intra-articular delivery of purified mesenchymal stem cells from C57BL/6 or MRL/MpJ superhealer mice prevents post-traumatic arthritis

Brian O. Diekman[1,2], **Chia-Lung Wu**[1,2], **Craig R. Louer**[1], **Bridgette D. Furman**[1], **Janet L. Huebner**[3], **Virginia B. Kraus**[3], **Steven A. Olson**[1], and **Farshid Guilak**[1,2,*]

[1]Department of Orthopaedic Surgery, Duke University Medical Center

[2]Department of Biomedical Engineering, Duke University

[3]Department of Medicine, Duke University Medical Center

Abstract

Joint injury dramatically enhances the onset of osteoarthritis (OA) and is responsible for an estimated 12% of OA. Post-traumatic arthritis (PTA) is especially common after intraarticular fracture, and no disease-modifying therapies are currently available. We hypothesized that the delivery of mesenchymal stem cells (MSCs) would prevent PTA by altering the balance of inflammation and regeneration after fracture of the mouse knee. Additionally, we examined the hypothesis that MSCs from the MRL/MpJ (MRL) "superhealer" mouse strain would show increased multilineage and therapeutic potentials as compared to those from C57BL/6 (B6) mice, as MRL mice have shown exceptional in vivo regenerative abilities. A highly purified population of MSCs was prospectively isolated from bone marrow using cell surface markers ($CD45^-$/$TER119^-$/$PDGFR\alpha^+$/$Sca\text{-}1^+$). B6 MSCs expanded greater than 100,000 fold in three weeks when cultured at 2% oxygen and displayed greater adipogenic, osteogenic, and chondrogenic differentiation as compared to MRL MSCs. Mice receiving only a control saline injection after fracture demonstrated PTA after 8 weeks, but the delivery of 10,000 B6 or MRL MSCs to the joint prevented the development of PTA. Cytokine levels in serum and synovial fluid were affected by treatment with stem cells, including elevated systemic interleukin-10 at several time points. The delivery of MSCs did not reduce the degree of synovial inflammation but did show increased bone volume during repair. This study provides evidence that intra-articular stem cell therapy can prevent the development of PTA after fracture and has implications for possible clinical interventions after joint injury before evidence of significant OA.

Keywords

Mesenchymal Stem Cells; Osteoarthritis; Post-traumatic arthritis; Intra-articular Fracture; Cell therapy; Immunomodulation

Copyright © 2012 Cognizant Communication Corporation

*Corresponding author: Farshid Guilak 375 Medical Sciences Research Bldg., Box 3093 DUMC, Durham, NC 27710 Phone: 919-684-2521 Fax: 919-681-8490 guilak@duke.eduhttp://ortho.duhs.duke.edu.

DISCLOSURE OF POTENTIAL CONFLICTS OF INTEREST: The authors have nothing to disclose.

NIH-PA Author Manuscript
NIH-PA Author Manuscript
NIH-PA Author Manuscript

NIH-PA Author Manuscript

NIH-PA Author Manuscript

NIH-PA Author Manuscript

INTRODUCTION

An estimated 27 million Americans have clinical osteoarthritis (OA) (45), and the risk of OA increases 10- to 20-fold following joint trauma such as ligament injury, meniscal tear, or intra-articular fracture (2). Post-traumatic arthritis (PTA) represents 12% of lower-extremity OA cases and causes a large economic burden due to the young age of the PTA population (8). The presence of inflammatory cytokines such as interleukin-1 (IL-1) and tumor necrosis factor α (TNF-α) in the joint fluid, synovium and other joint tissues has emerged as an important contributor to the pathogenesis of both idiopathic and secondary OA (5,15,23,27,32,33). Furthermore, the rapid development of OA after closed-joint intraarticular fracture of the mouse knee has confirmed the central role of inflammation and provides a model system for examining the effects of different therapeutic approaches to prevent the onset or progression of PTA (22,24,50).

The delivery of mesenchymal stem cells (MSCs) has been proposed as a regenerative therapy for a wide range of disease states. An emerging paradigm suggests that long-term engraftment and differentiation may not be the primary regenerative mechanisms of exogenously delivered MSCs. Instead, MSCs modulate inflammation and provide a regenerative environment either by direct secretion of bioactive factors, or by altering the cytokine and growth factor production of endogenous cells (9,39,63,66). In several models of disease, MSCs exert protective effects by producing anti-inflammatory molecules such as IL-1 receptor antagonist (IL-1ra) and interleukin-10 (IL-10) (59,60). While stem cell based solutions have been studied for musculoskeletal repair and regeneration (3,46,58,73), MSC therapy for the prevention of PTA after closed intra-articular fracture has not been investigated.

Different mouse strains possess significantly different regenerative phenotypes, suggesting that their MSCs may have different therapeutic effectiveness. For example, the MRL/MpJ (MRL) “superhealer” inbred mouse strain has shown enhanced regeneration after injury in a variety of tissues such as the ear, cornea, heart, digit tips, and articular cartilage (11,12,20,48,76). Of particular interest was the observation that MRL mice were protected from PTA after intra-articular fracture (80). Regeneration in MRL mice is correlated with a reduced inflammatory signature after injury (22,28,36,52), suggesting an altered transition from the acute inflammatory phase to a resolution phase that allows for regeneration. The contribution of MSCs to this transition is unknown, but bone-marrow derived MSCs from MRL mice exhibited enhanced engraftment, deposition of granulation tissue, and functional improvement in a model of myocardial injury (1).

The evaluation of MSC therapy in pre-clinical models is hampered by the technical challenges associated with in vitro culture of murine MSCs, such as slow expansion and the persistence of contaminating cell populations (62). Strategies to overcome these limitations have included extended culture periods at low density (56,61), removing undesired cell types by modified plating techniques or immunodepletion (4,72,74), expanding cells in hypoxic conditions (71), or utilizing compact bone as an enriched MSC source as compared to bone marrow (71,81,84). In recent studies, Morikawa et al. reported a method for prospectively isolating a pure population of bone marrow-derived MSCs utilizing collagenase digestion and flow cytometry cell sorting for cells co-expressing platelet derived growth factor receptor α (PDGFRα, also known as CD140a) and stem cell antigen-1 (Sca-1) (57). In this study, we found that culturing PDGFRα^+/Sca-1^+ MSCs at low oxygen tension greatly increased the rate of cell proliferation, thus providing a pure and extensive source of murine MSCs with multi-lineage potential.

NIH-PA Author Manuscript

NIH-PA Author Manuscript

NIH-PA Author Manuscript

We hypothesized that the delivery of MSCs directly to the joint space after fracture would prevent the development of PTA by altering the inflammatory environment. Additionally, we used this model system to compare the regenerative capabilities of MSCs isolated from control C57BL/6 mice and MRL/MpJ “superhealer” mice.

MATERIALS AND METHODS

MSC Isolation

All procedures were performed in accordance with a protocol approved by the Duke University Institutional Animal Care and Use Committee. For stem cell isolation, male MRL/MpJ (The Jackson Laboratory, Bar Harbor, ME) or C57BL/6 (Charles River Laboratories, Wilmington, MA) mice were sacrificed at 8–10 weeks of age with CO_2. Excised femurs and tibias were crushed into fragments and the exposed bone marrow was gently removed by washing. Digestion with 5 ml of 0.2% collagenase type I (Worthington Biochemical, Lakewood, NJ) per mouse for 60 minutes at 37 °C released cells that were filtered through a 70 μm strainer (BD biosciences, San Jose, CA) and treated with ACK buffer to lyse erythrocytes. Cells were treated with Fc block and labeled with antibodies to mouse CD45 (fluorescein isothiocyanate [FITC]), TER-119 (FITC), Sca-1 (Alexa 647), and PDGFRα (phycoerythrin [PE]) or isotype controls for 30 minutes at 4 °C (all from Biolegend, San Diego, CA). A Cytomation MoFlo® sorter (Beckman Coulter, Bray, CA) captured cells negative for CD45/TER-119 and positive for both Sca-1 and PDGFRα (57).

MSC Expansion

After sorting, MSCs were cultured at 100 cells/cm^2 in expansion medium consisting of alpha modified Eagle's medium (αMEM; Invitrogen, Carlsbad, CA), 20% lot-selected fetal bovine serum (FBS; Sigma-Aldrich, St Louis, MO), and 1% penicillin/streptomycin/fungizone (P/S/F, Invitrogen) in a hypoxic incubator (37 °C, 2% O_2, 5% CO_2, remaining gas N_2). After 8 days with media changes every 3 days, cells were passaged and plated at 3000 cells/cm^2 with subsequent passages carried out every 3–4 days upon 90% confluence. Expansion rates were calculated from three independent isolations of 3–6 mice of each strain.

Colony-forming unit (CFU-F) assay

Two-hundred fifty freshly sorted MSCs were plated in wells of a 6 well plate (9.5 cm^2) in expansion medium. After 7 days with no medium changes, wells were stained with 3% crystal violet, washed repeatedly with PBS, and then analyzed for defined colonies of greater than 10 cells using standard microscopy, with data presented from three wells of one of two independent experiments.

Flow cytometry

Passage 3 cells were treated with Fc block and labeled with antibodies to the following cell surface markers and appropriate isotype controls (all from Biolegend): mouse CD45 (FITC), CD49d (FITC), TER-119 (FITC), CD44 (PE-Cyanine 5 [Cy5]), CD29 (PE-Cy5), C-X-C chemokine receptor type 4 (CXCR4; Alexa 647), CD11b (allophycocyanin [APC]), PDGFRα (PE), Sca-1 (Alexa 647). A C6 benchtop flow cytometer (Accuri Cytometers, Ann Arbor, MI) was used for analysis and percentages obtained by subtracting the value of isotype controls.

Adipogenic differentiation

Ten thousand cells at passage 2–3 were plated in wells of 48 well plates (0.95 cm^2) for 2 days in expansion medium at normoxic conditions. Media was then switched to control

NIH-PA Author Manuscript

NIH-PA Author Manuscript

NIH-PA Author Manuscript

medium consisting of Dulbecco's modified Eagle Medium/F12 (DMEM/F12; Lonza, Walkersville, MD) with 3% FBS and 1% P/S/F or adipogenic differentiation medium (34) consisting of control medium plus (all from Sigma-Aldrich) 33 μM biotin, 17 μM pantothenate, 1 μM bovine insulin, 1 μM dexamethasone, and for the first three days only 250 μM isobutylmethylxanthine (IBMX) and 2 μM rosiglitazone (Avandia™). After 14 days, cells were imaged and then fixed with 4% paraformaldehyde. Monolayers were stained as described (34) with 0.5% Oil Red O stain (EMD Chemicals, Gibbstown, NJ). Cells were washed with 60% isopropanol and the stain was released with 250 μl of 100% isopropanol and then quantified by absorbance at 535 nm, with data presented from three wells of one of two independent experiments.

Osteogenic differentiation

Ten thousand cells at passage 2–3 were plated in wells of 48 well plates (0.95 cm^2) for 2 days in expansion medium at normoxic conditions. Media was then switched to control medium consisting of DMEM-high glucose (HG) with 10% FBS and 1% P/S/F or osteogenic differentiation medium (79) consisting of control medium plus 10 mM β-glycerophosphate (Sigma-Aldrich), 250 μM ascorbate (Sigma-Aldrich), 2.5 μM retinoic acid (Sigma-Aldrich), and 50 ng/ml human bone morphogenetic protein-2 (BMP-2, R&D systems, Minneapolis, MN). After 21 days, cells were fixed with 4% paraformaldehyde and stained with 2% Alizarin Red S (Electron Microscopy Sciences, Hatfield, PA) for 20 minutes. After two washes with deionized water, wells were photographed and then Alizarin stain was released for quantification by heated acid extraction (31). Briefly, 10% v/v acetic acid was added to well for 30 minutes at room temperature and then transferred to Eppendorfs for 10 minutes at 85 °C. Ammonium hydroxide (10% v/v) was added to neutralize the acid and absorbance was measured at 405 nm, with data presented from five wells of one of two independent experiments.

Chondrogenic differentiation

Two hundred fifty thousand cells at passage 2–3 in expansion medium were placed in 15 ml polypropylene tubes and centrifuged at 300 × g for 5 minutes to form rounded pellets. After 2 days, media was switched to serum free control medium consisting of DMEM-HG (Invitrogen), 1% insulin transferrin insulin + (ITS+; BD), 50 μg/ml ascorbate (Sigma-Aldrich), 40 μg/ml proline (Sigma-Aldrich), and 1% P/S/F (Sigma-Aldrich) or chondrogenic differentiation medium (16) consisting of control medium plus 10 ng/ml human transforming growth factor-β3 (TGF-β3, R&D) and 500 ng/ml human bone morphogenetic protein-6 (BMP-6, R&D). After 28 days, pellets were processed for Safranin-O/Fast Green histological staining or biochemical analysis by measuring double stranded DNA with the PicoGreen assay and glycosaminoglycan (GAG) content with the 1,9 dimethylmethylene blue (DMB) assay as previously described (17). Data presented are from three or more pellets of one of two independent experiments.

Intra-articular fracture

B6 mice at the skeletally mature age of 16 weeks were used for a closed tibial plateau fracture model of PTA as previously described (24,80). Briefly, the sedated mouse was fit into a custom cradle so that the left hind limb was at neutral position under a 10 N preload, which was applied using a wedge-shaped indenter attached to a materials testing system (ElectroForce ELF3200, Bose Corp., Minnetonka MN). Compression force was applied until −2.7 mm displacement at a rate of 20 N/s in load control. Each fracture was confirmed using high resolution digital X-ray (MX-20, Faxitron, Lincolnshire, IL). Right hind limbs were not fractured and served as contralateral controls. Fifty-one mice received fractures of the left hind limb, while right hind limbs were not fractured and served as contralateral controls.

NIH-PA Author Manuscript

NIH-PA Author Manuscript

NIH-PA Author Manuscript

Stem cell injection

MSCs were pooled from six B6 or MRL mice and expanded three passages in monolayer culture. MSCs were delivered immediately after fracture. The sedated mice were injected with either sterile saline only (Hospira Inc, Lake forest, IL) or 10,000 MSCs in 6 μl saline using a specialty syringe (catalog #80401, Hamilton Company, Reno, NV) and 30 ga ½ needle (BD). The mouse was positioned for lateral entry with the left hind limb extended to facilitate injection of 6 μl into the joint space through the patellar tendon. This delivery technique does not result in initiation of osteoarthritis (77). To allow for cell tracking, some MSCs were first treated with 4 μM of the membrane dye chloromethylbenzamido (CM-DiI, Sigma-Aldrich) for 5 minutes and washed before injection.

Serum and synovial fluid analysis

Retro-orbital bleeding and cardiac stick were used to collect blood at the time of sacrifice, with three mice for pre-fracture controls, day 1, day 3, and day 7 time points, and eight mice for 8 weeks after fracture and injection. After clotting, samples were centrifuged at 3500 rpm for 15 minutes and serum was transferred to −80 °C. At the same time points, synovial fluid from fractured and contralateral limbs was isolated from the exposed joint space as previously described (70). Briefly, the synovial fluid was absorbed onto a Melgisorb pad and this was dissolved with 35 μl alginate lyase and 15 μl sodium citrate. Serum and synovial fluid from the fractured knee were analyzed for the presence of the following cytokines by ELISA utilizing the manufacturer's instructions and a 1:5 dilution for synovial fluid samples (R&D Systems): IL-1β (cat #MLB00C), interleukin-1 receptor antagonist (IL-1ra, cat #MRA00), and interleukin-10 (IL-10, cat #M1000, serum only). Samples that were undetectable were assigned a value of one half of the lower limit of quantification for analysis.

Analysis of mouse joints

Eight weeks after fracture, eight mice per group were sacrificed and both fractured and contralateral control limbs were fixed in neutral alignment using 10% neutral buffered formalin for 48 hours. Joints were transferred to 70% ethanol and analyzed with micro-computed tomography (μCT 40, Scanco Medical, Brüttisellen, Switzerland) as previously described (24,80). Briefly, transverse slices of 16 μm were used to generate 3D reconstructions that were subjected to global threshholding to separate bone from soft tissue. A phantom was used to calibrate linear attenuation to hydroxyapatite (HA) concentration for bone density measurements. Bone density and bone volume were analyzed from eight mice per group in three regions: cancellous bone of the distal femoral condyles, tibial plateau distal to subchondral plate, and metaphyseal region of tibial plateau. After micro-CT analysis, the limbs were decalcified and processed for histology using an increasing ethanol series, xylenes, and paraffin steps in an automated tissue processor (ASP300S, Leica Microsystems, Buffalo Grove, IL).

Coronal plane sections of 8 μm were taken for histology and stained with Safranin-O/Fast-green/Hematoxylin for analysis of cartilage degradation. Modified Mankin grading of OA features including changes to cartilage structure and loss of Safranin-O staining was performed by three blinded graders and used to calculate a score with a maximum of 30 for both the medial and lateral aspects of the femur and tibia (23). Sections were stained with Harris hematoxylin and eosin (H&E) for assessment of synovitis by three blinded graders as previously described (22). One joint was unable to be processed, leaving at least seven mice for each group for modified Mankin and synovitis grading. Three selected joints from each group were analyzed with immunohistochemistry for activated macrophages using a monoclonal antibody against F4/80 (Clone BM8, Biolegend). Antigen retrieval was aided by 0.05% Proteinase K (Sigma-Aldrich) and heated citrate buffer extraction. Chromogen

NIH-PA Author Manuscript

NIH-PA Author Manuscript

NIH-PA Author Manuscript

detection was carried out with the Vectastain system (Vector Laboratories, Burlingame, CA). For one mouse per group at each time point, sections were analyzed for CM-DiI cell tracking by clearing with xylenes and exciting with a 543 nm laser using confocal microscopy (LSM510, Zeiss, Peabody, MA).

Statistical analysis

Statistical analysis was carried out using a *t*-test for comparison of two groups and analysis of variance (ANOVA) for comparison of multiple groups, with repeated measures ANOVA on control and fractured limbs for modified Mankin scoring. Fisher's LSD post-hoc analysis with α=0.05 was used. Normality was tested and data log-transformed before analysis if necessary. For non-parametric analysis of cytokine data, undetectable values were assigned the value of one half of the lower limit of detection for analysis. Kruskal-Wallis Median test was used to determine the effect of time point and the main effects of treatment group at each time point. Data are presented as mean ± standard error of the mean.

RESULTS

Rapid expansion of purified MSCs

Bone marrow-derived MSCs were isolated from B6 and MRL mice by utilizing collagenase digestion and the expression of specific cell surface markers. While the percentage of bone marrow cells expressing hematopoietic lineage markers varied with each isolation, a representative isolation shows 0.70% of all cells were negative for the hematopoietic markers CD45 and TER-119, and 5.09% of these cells were positive for both PDGFRα and Sca-1 (Figure 1A). B6 and MRL mice contained a similar number of MSCs, with yields of approximately 300–600 MSCs per mouse. Within the sorted MSC population, MRL mice had a higher frequency of colony forming cells as assessed by the CFU-F assay (19 ± 1.15 vs. 10 ± 0.58 colonies per 250 starting cells, $p<0.05$).

MSCs were expanded in a 2% O_2 environment. Individual colonies of B6 MSCs were established at day 4 (Figure 1B), grew significantly by day 6 (Figure 1C), and continued to proliferate at passage 3 (Figure 1D), with similar results for MRL MSCs (Figure 1E–G). MSCs from B6 mice showed a trend toward greater expansion as compared to MRL mice (Figure 1H), resulting in a 13-fold higher cumulative fold increase in cell number at the end of 3 passages (154,141 ± 113,095 vs. 11,728 ± 5069 cells per starting cell, $p>0.05$).

Characterization of MSCs from B6 and MRL mice

Passage 3 MSCs from both strains displayed cell surface markers consistent with previous MSC isolation strategies such as being uniformly positive for CD44 and Sca-1 (>95%) and uniformly negative for CD11b (<1%). MSCs were also negative for cell surface markers related to homing capabilities (<1% for CD49d, <1% for CXCR4). MSCs retained expression of PDGFRα in culture although not uniformly (91.4% of B6 and 81.9% of MRL).

MSCs differentiated into cells with the properties of adipocytes, osteoblasts, and chondrocytes (Figure 2). In general, B6 MSCs demonstrated enhanced differentiation as compared to MRL MSCs. After 14 days in adipogenic media, more lipid droplets formed in B6 MSC cultures (Figure 2 A,B) and quantification by release of lipid staining showed a significant increase in adipogenesis as compared to MRL MSCs (0.11 ± 0.005 vs. 0.092 ± 0.005 absorbance units, $p<0.05$, Figure 2C). B6 MSCs also demonstrated a trend toward increased osteogenesis (Figure 2D) as compared to MRL MSCs (Figure 2E) when quantified by heated extraction of Alizarin S mineralization staining (0.73 ± 0.26 vs. 0.22 ± 0.064 adjusted absorbance units, $p=0.13$, Figure 2F). Chondrogenesis was assessed by the

NIH-PA Author Manuscript

NIH-PA Author Manuscript

NIH-PA Author Manuscript

production of GAGs after 28 days of pellet culture (Figure 2G,H). B6 MSC pellets contained more GAGs than MRL MSCs (68.65 ± 1.23 vs. 20.25 ± 0.077 μg per pellet, $p<0.05$, Figure 2I) despite a smaller overall pellet size.

Prevention of post-traumatic arthritis by stem cell therapy

Fracture of the left hind limb treated with only a control saline injection resulted in a significantly higher modified Mankin osteoarthritis score as compared to the contralateral control limb, indicating the presence of PTA in this group of mice (Figure 3A). Direct intra-articular delivery of either B6 or MRL MSCs immediately after fracture eliminated the difference in total joint modified Mankin score between the fractured limb and the control limb, showing MSC therapy was able to mitigate the development of PTA. Due to the location of the fracture, degeneration was most severe at the lateral tibia and the protective effect of the MSC therapy was most apparent on the lateral side of the joint (Figures 3B–D). A small number of MSCs were detected in various joint structures at days 1, 3, 7 as well as 8 weeks (Figure 4).

Serum and synovial fluid analysis

The level of IL-1β in serum was increased at early time points after fracture and returned towards the pre-fracture values after 8 weeks in all groups with no significant effect of treatment (Figure 5A). The treatment group did have a significant effect on synovial fluid levels of IL-1β at day 3 and at 8 weeks, with MSC treatment being associated with higher values at day 3 but reduced levels at 8 weeks (Figure 5B). Serum levels of IL-1ra were affected by the treatment group at 8 weeks, with elevated IL-1ra in the B6 MSC treatment group (Figure 5C), and all groups demonstrated a trend towards increased synovial fluid IL-1ra 7 days after fracture (Figure 5D). The treatment group significantly affected the serum levels of IL-10 at days 3 and 7 after fracture, with higher values in the MSC treated groups (Figure 5E).

Synovial inflammation and macrophage immunohistochemistry

The inflammation of the synovium 8 weeks after fracture was measured by a synovitis score that assesses the thickening of the synovial lining as well as the cellularity of the surrounding stroma. Fracture clearly increased the degree of synovitis in all treatment groups as compared to the contralateral control and MRL MSCs resulted in more inflammation than B6 MSCs (Figure 6A). The typical synovial lining of 1–2 cell layers (Figure 6B) showed extensive thickening after fracture (Figure 6C). An antibody against F4/80, used to identify activated macrophages, demonstrated that some of the cells contributing to the synovial response are macrophages (Figure 6D). No clear differences in macrophage staining were apparent between treatment groups.

Morphologic bone changes

Micro-CT analysis of morphologic bone changes showed increased bone volume and decreased bone density in the tibia and tibial metaphysis of the fractured limb as compared to the contralateral control limb (Figure 7). The stem cell groups appeared to contribute to a larger bone volume, with the fractured limbs receiving MRL MSCs having a significantly larger volume than all control limbs in the tibial metaphysis (Figure 7C). In the femur, the saline group showed significantly lower cancellous bone fraction (bone volume / total volume) in the fractured limb compared to the control limb and compared to both MSC therapy groups (Figure 7E). With MSC treatment, there was no significant decrease in cancellous bone fraction following fracture as compared to the contralateral control limbs.

NIH-PA Author Manuscript

NIH-PA Author Manuscript

NIH-PA Author Manuscript

DISCUSSION

The goal of this study was to prevent the development of OA after intra-articular fracture using a single injection of expanded MSCs directly into the murine knee joint. Our findings show that an allogeneic stem cell based therapy can prevent the degenerative changes following joint trauma, and similar protective effects were observed using either B6 or MRL MSCs. The modified Mankin score of the fractured joint was significantly higher than the control joint when only saline was used as the treatment, indicative of PTA. However, intra-articular injection of 10,000 B6 or MRL MSCs after fracture eliminated the difference between control and fractured limbs. Establishing treatment options for PTA is particularly promising because, in contrast to idiopathic OA, the clear initiating event allows for early intervention before excessive degradation occurs (2).

We confirmed that prospective isolation of PDGFRα^+/Sca-1$^+$ cells from bone marrow results in a highly purified population of MSCs, with approximately one out of twenty cells undergoing clonal expansion, as compared to the one out of one million typically achieved from unsorted mouse bone marrow (62). A novel and important finding of this study was that expansion in 2% oxygen culture substantially increased the proliferation rate of this cell population. In just 3 weeks, purified MSCs from B6 mice expanded greater than 100,000 fold as compared to the reported value of 10,000 fold expansion over 3 months when cultured at normoxia (57). This finding is consistent with previous studies showing low oxygen tension facilitates human, rat, and mouse MSC expansion (6,13,30,49,71,75) by providing oxygen tension levels that are more representative of the in situ bone marrow microenvironment (38).

The use of cellular therapy or cell-based tissue engineering for the regeneration of cartilage after joint injury has generated promising pre-clinical and case study results. With regard to PTA, the intra-articular delivery of MSCs has been shown to lessen the degree of OA in goat knees after meniscectomy and ACL resection, potentially through partial regeneration of the resected mensicus (58). Recent studies have also shown a protective effect of infrapatellar fat pad cells injected in the rabbit knee following transection of the ACL (73). Furthermore, a series of studies in mice and rats demonstrated that delivery of BMP-2 overexpressing stem cells contributed to fracture healing and cartilage repair after open osteotomy of the hind limb (82,83). There are currently 8 clinical trials investigating the injection of MSCs for osteoarthritis (55), including a phase I/II clinical trial to prevent OA after meniscal tear (http://clinicaltrials.gov, #NCT00702741). In a related approach, clinical case studies have shown the ability of MSCs to produce neotissue when combined with a collagen gel and placed in cartilage defects (54,78).

The concept that MSCs may prevent PTA after intra-articular fracture is consistent with the role of endogenous stem cells after bone and cartilage injury. After long-bone fracture, MSCs arrive at the fracture site to instigate endochondral ossification as part of the repair process (reviewed in Marsell & Einhorn (53)). A similar mechanism is likely to occur after intra-articular fracture, as a multipotent MSC population was derived from hemarthrosis in joints after fracture (47). Indeed, treatment of chondral defects with microfracture or other marrow stimulating techniques relies on accessing the subchondral bone marrow to allow infiltration of progenitor cells (21,41,67).

Cytokines such as IL-1β are upregulated with joint trauma (37,64) and result in cartilage degradation by suppressing matrix synthesis and inducing catabolic matrix metalloproteinase (MMP) activity (18,27). In contrast, increased systemic or joint levels of IL-1ra may disrupt the inflammatory cascade by preventing IL-1 from binding to its cell receptor (10,44).

NIH-PA Author Manuscript

NIH-PA Author Manuscript

NIH-PA Author Manuscript

Similarly, IL-10 has been identified as an important anti-inflammatory molecule that shows a chondroprotective role in several settings of joint disease (reviewed in Schulze-Tanzil et al. (69)). We hypothesized that MSC therapy would preserve cartilage by altering the balance of these pro-inflammatory and anti-inflammatory cytokines in the joint after injury. In studies using other injury models, MSCs decreased the systemic level of IL-1β after long-bone fracture (29), protected the lung from injury by secreting IL-1ra (60), and reprogrammed macrophages to increase IL-10 production in a sepsis model (59). In this study, stem cell treatment altered the levels of IL-1β in the synovial fluid and the presence of IL-10 in the serum at several time points. However, serum levels of IL-1β were not affected by treatment group, indicating that the strong systemic inflammatory response at early time points after fracture is not eliminated by MSC therapy.

The synovium is a likely target for the therapeutic effects of MSCs because it exhibits significant cellular activity in response to injury. However, the relationship between stem cells and the synovium is complex, as endogenous MSCs in the mouse synovium contribute to a regenerative response through chondrogenic differentiation after cartilage injury (43), but a significant inflammatory environment can alter the differentiation of progenitors in the synovium and cause a pannus-like invasion (51). Inflammation of the synovium after injury is correlated to negative outcomes in clinical studies of meniscal injury (68). Synovitis was clearly caused by fracture in this study, but stem cell therapy improved OA scores without reducing the degree of synovial hyperplasia after fracture. Since macrophages have been implicated as producers of inflammatory cytokines and other destructive molecules such as MMPs (5), we performed immunohistochemical staining for activated macrophages. Similar to the overall synovial inflammation, delivery of MSCs did not appear to mitigate the presence of activated macrophages in the synovium. However, MSCs were capable of inhibiting the proliferation of in vitro stimulated splenocytes (data not shown), consistent with their proposed immunomodulatory function (reviewed in Ghannam et al. (26)).

Bone is a joint tissue with high turnover and the capacity to respond to MSC delivery. In a long-bone fracture model, systemically delivered MSCs produced BMP-2 at the fracture site and caused an increase in callus strength, total volume, and mineralization content (29). In this study, MSCs directly delivered to the joint increased several measures of bone volume. The finding that MSC therapy prevents the decrease in bone volume to total volume ratio in the femur after fracture of the tibia suggests an influence on PTA development as opposed to enhanced healing at the fracture site only. Exogenously delivered MSCs may contribute to the prevention of PTA by providing additional cells for earlier and more robust stabilization of the joint, thus affecting the function and loading of the limb. The differentiation of endogenous MSCs to an osteoblastic lineage is essential to bone repair and is organized by multiple waves of biochemical signals such as IL-1 and TNFα (53). Since these inflammatory cytokines are essential to early fracture healing but may be catabolic for cartilage at later times, the timing and dose of MSCs or other agents that may affect cytokine levels will need to be considered for optimal fracture repair and protection from PTA.

There is controversy in the literature about the extent of MSC engraftment when used in injury models, with some studies showing significant engraftment and differentiation but most demonstrating functional improvements with few cells remaining at the site of cell delivery (reviewed in Prockop (65)). With systemic delivery, MSCs get trapped in the lungs before distribution to organs such as the liver and spleen (25). However, intra-articular delivery of stem cells to the knee has resulted in some engraftment in joint structures (35,46,58). For cell tracking experiments, we labeled cells with CM-DiI, which is a lipophilic carbocyanine membrane dye that has been used effectively for tracking cells in vivo in the context of bone (19). Consistent with previous studies, we observed a relatively small fraction of fluorescent cells in various tissues of the joint throughout the time course

NIH-PA Author Manuscript

NIH-PA Author Manuscript

NIH-PA Author Manuscript

studied. However, quantification was not possible due to the challenges associated with discriminating between infrequent positive cells and background fluorescence (7) and the possibility of membrane dyes transferring to other cells over a period of time (42). New methods for quantifying the rate of engraftment and longitudinally tracking the fate of delivered cells will be an important aspect for the future development of cellular therapies (14).

The identification of MSCs with exceptional properties can help elucidate how the cells contribute to healing and may provide a pathway to modify MSCs for enhanced function. Because MRL "superhealer" mice may derive some of their regenerative capabilities from altered stem cell function (1), MSCs from both control B6 and MRL mice were compared in this model system. Our hypothesis was that MSCs isolated from MRL mice would demonstrate distinct in vitro characteristics and improved therapeutic effectiveness in vivo when compared to B6 MSCs. We found that although MRL MSCs had a higher frequency of clonogenic cells, these cells have lower expansion rates as compared to B6 MSCs. This finding was surprising given that Alfaro et al showed enhanced proliferation of MSCs from MRL mice (1). This discrepancy may be due to differences either in isolation or expansion procedures. We used PDGFRα^+/Sca-1$^+$ sorting of cells after collagenase digestion as opposed to immunodepletion of flushed bone marrow cells for isolation, and we expanded the cells at 2% oxygen as opposed to normoxia, resulting in a much higher rate of proliferation. Regardless, the relationship between in vitro proliferation rates and in vivo functionality is unclear. While rapid expansion of MSCs is desired for in vitro studies, MSCs are typically quiescent in vivo until activated as demonstrated by the finding that 71% of freshly isolated PDGFRα^+/Sca-1$^+$ MSCs are in the G0 phase (57).

Previous studies have shown enhanced repair of cartilage defects in MRL mice as compared to B6 mice, but only if the injury extended through the subchondral bone (20). These findings led us to hypothesize that the unique regenerative potential of MRL mice may arise from a superior differentiation potential of their MSCs. Contrary to this hypothesis, B6 MSCs displayed more robust differentiation down the adipogenic, osteogenic, and chondrogenic lineage than MRL MSCs. This difference was not caused by proliferation during differentiation, as the trends remained the same when data were normalized to cell number (data not shown).

The cellular therapy experiments demonstrated similar results using MSCs from either B6 or MRL mice. One explanation is that delivering exogenous stem cells of either strain to the B6 knee after fracture is sufficient to reduce inflammation and create a joint environment that is protected from PTA, as seen with MRL mice after fracture (22,80). This is supported by work showing that MRL mice had different serum and synovial fluid IL-1β profiles after fracture (22) and that macrophages from MRL mice have lower upregulation of inflammatory cytokines (40). Indeed, experiments investigating the ear wound closure of MRL mice demonstrated that the regenerative phenotype of MRL mice is lost when the inflammatory environment is changed due to a secondary injury (85). Interestingly, there was a non-significant trend towards increased cartilage degradation of the non-fractured control limb with MSC therapy as compared to saline treatment, suggesting that the influence of intraarticular MSC therapy may extend to systemic effects. However, this trend may also be related to MSC therapy protecting the fractured limb from PTA and therefore affecting activity levels, although this was not investigated in this study.

CONCLUSIONS

We demonstrated that a single intra-articular injection of MSCs from either control B6 or MRL "superhealer" mice prevented the development of post-traumatic arthritis 8 weeks

NIH-PA Author Manuscript

NIH-PA Author Manuscript

NIH-PA Author Manuscript

after intra-articular fracture of the knee. MSCs did not reduce synovitis or the presence of activated macrophages in the synovium, but did alter cytokine levels and the bone healing response. This work suggests that stem cell therapy is a promising treatment for preventing PTA and could possibly be extended to explore other biologic interventions after joint injury before extensive osteoarthritis has occurred.

Acknowledgments

The authors thank Nancy Martin and Dr. Mike Cook of the Flow Cytometry Shared Resource of the Duke Cancer Institute, as well as Stephen Johnson, Evan Zeitler and Elisabeth Flannery for contributions to this work. Funding from NIH AR50245, AR48852, AG15768, AR48182, NSF Graduate Research Fellowship (BOD), and the Arthritis Foundation.

REFERENCES

1. Alfaro MP, Pagni M, Vincent A, Atkinson J, Hill MF, Cates J, Davidson JM, Rottman J, Lee E, Young PP. The Wnt modulator sFRP2 enhances mesenchymal stem cell engraftment, granulation tissue formation and myocardial repair. Proc. Natl. Acad. Sci. USA. 2008; 105(47):18366–18371. [PubMed: 19017790]
2. Anderson DD, Chubinskaya S, Guilak F, Martin JA, Oegema TR, Olson SA, Buckwalter JA. Post-traumatic osteoarthritis: Improved understanding and opportunities for early intervention. J. Orthop. Res. 2011; 29(6):802–809. [PubMed: 21520254]
3. Arthur A, Zannettino A, Gronthos S. The therapeutic applications of multipotential mesenchymal/stromal stem cells in skeletal tissue repair. J. Cell. Physiol. 2009; 218(2):237–245. [PubMed: 18792913]
4. Baddoo M, Hill K, Wilkinson R, Gaupp D, Hughes C, Kopen GC, Phinney DG. Characterization of mesenchymal stem cells isolated from murine bone marrow by negative selection. J. Cell. Biochem. 2003; 89(6):1235–1249. [PubMed: 12898521]
5. Bondeson J, Blom AB, Wainwright S, Hughes C, Caterson B, van den Berg WB. The role of synovial macrophages and macrophage-produced mediators in driving inflammatory and destructive responses in osteoarthritis. Arthritis Rheum. 2010; 62(3):647–657. [PubMed: 20187160]
6. Boregowda SV, Krishnappa V, Chambers JW, Lograsso PV, Lai WT, Ortiz LA, Phinney DG. Atmospheric Oxygen Inhibits Growth and Differentiation of Marrow-Derived Mouse Mesenchymal Stem Cells via a p53-Dependent Mechanism: Implications for Long-Term Culture Expansion. Stem Cells. 2012; 30(5):975–987. [PubMed: 22367737]
7. Brazelton TR, Blau HM. Optimizing techniques for tracking transplanted stem cells in vivo. Stem Cells. 2005; 23(9):1251–1265. [PubMed: 16109764]
8. Brown TD, Johnston RC, Saltzman CL, Marsh JL, Buckwalter JA. Posttraumatic osteoarthritis: a first estimate of incidence, prevalence, and burden of disease. J. Orthop. Trauma. 2006; 20(10):739–744. [PubMed: 17106388]
9. Caplan AI, Dennis JE. Mesenchymal stem cells as trophic mediators. J. Cell. Biochem. 2006; 98(5):1076–1084. [PubMed: 16619257]
10. Caron JP, Fernandes JC, Martel-Pelletier J, Tardif G, Mineau F, Geng C, Pelletier JP. Chondroprotective effect of intraarticular injections of interleukin-1 receptor antagonist in experimental osteoarthritis. Suppression of collagenase-1 expression. Arthritis Rheum. 1996; 39(9):1535–1544. [PubMed: 8814066]
11. Chadwick RB, Bu L, Yu H, Hu Y, Wergedal JE, Mohan S, Baylink DJ. Digit tip regrowth and differential gene expression in MRL/Mpj, DBA/2, and C57BL/6 mice. Wound Repair Regen. 2007; 15(2):275–284. [PubMed: 17352761]
12. Clark LD, Clark RK, Heber-Katz E. A new murine model for mammalian wound repair and regeneration. Clin. Immunol. Immunopathol. 1998; 88(1):35–45. [PubMed: 9683548]
13. Das R, Jahr H, van Osch GJ, Farrell E. The role of hypoxia in bone marrow-derived mesenchymal stem cells: considerations for regenerative medicine approaches. Tissue. Eng. Part B Rev. 2010; 16(2):159–168. [PubMed: 19698058]

NIH-PA Author Manuscript

NIH-PA Author Manuscript

NIH-PA Author Manuscript

14. de Almeida PE, van Rappard JR, Wu JC. In vivo bioluminescence for tracking cell fate and function. Am. J. Physiol. Heart Circ. Physiol. 2011; 301(3):H663–671. [PubMed: 21666118]
15. Denoble AE, Huffman KM, Stabler TV, Kelly SJ, Hershfield MS, McDaniel GE, Coleman RE, Kraus VB. Uric acid is a danger signal of increasing risk for osteoarthritis through inflammasome activation. Proc. Natl. Acad. Sci. USA. 2011; 108(5):2088–2093. [PubMed: 21245324]
16. Diekman BO, Rowland CR, Lennon DP, Caplan AI, Guilak F. Chondrogenesis of adult stem cells from adipose tissue and bone marrow: induction by growth factors and cartilage-derived matrix. Tissue. Eng. Part A. 2010; 16(2):523–533. [PubMed: 19715387]
17. Estes BT, Diekman BO, Gimble JM, Guilak F. Isolation of adipose-derived stem cells and their induction to a chondrogenic phenotype. Nat. Protoc. 2010; 5(7):1294–1311. [PubMed: 20595958]
18. Fernandes JC, Martel-Pelletier J, Pelletier JP. The role of cytokines in osteoarthritis pathophysiology. Biorheology. 2002; 39(1–2):237–246. [PubMed: 12082286]
19. Ferrari A, Hannouche D, Oudina K, Bourguignon M, Meunier A, Sedel L, Petite H. In vivo tracking of bone marrow fibroblasts with fluorescent carbocyanine dye. J. Biomed. Mater. Res. 2001; 56(3):361–367. [PubMed: 11372053]
20. Fitzgerald J, Rich C, Burkhardt D, Allen J, Herzka AS, Little CB. Evidence for articular cartilage regeneration in MRL/MpJ mice. Osteoarthritis Cartilage. 2008; 16(11):1319–1326. [PubMed: 18455447]
21. Frisbie DD, Oxford JT, Southwood L, Trotter GW, Rodkey WG, Steadman JR, Goodnight JL, McIlwraith CW. Early events in cartilage repair after subchondral bone microfracture. Clin. Orthop. Relat. Res. 2003; (407):215–227. [PubMed: 12567150]
22. Furman, BD.; Huebner, JL.; Seifer, DR.; Kraus, VB.; Guilak, F.; Olson, SA. MRL/MpJ Mouse Shows Reduced Intra-Articular and Systemic Inflammation Following Articular Fracture. 55th Annual Meeting of the Orthopaedic Research Society; Las Vegas, NV. 2009. p. 1120
23. Furman BD, Olson SA, Guilak F. The development of posttraumatic arthritis after articular fracture. J. Orthop. Trauma. 2006; 20(10):719–725. [PubMed: 17106385]
24. Furman BD, Strand J, Hembree WC, Ward BD, Guilak F, Olson SA. Joint degeneration following closed intraarticular fracture in the mouse knee: a model of posttraumatic arthritis. J. Orthop. Res. 2007; 25(5):578–592. [PubMed: 17266145]
25. Gao J, Dennis JE, Muzic RF, Lundberg M, Caplan AI. The dynamic in vivo distribution of bone marrow-derived mesenchymal stem cells after infusion. Cells Tissues Organs. 2001; 169(1):12–20. [PubMed: 11340257]
26. Ghannam S, Bouffi C, Djouad F, Jorgensen C, Noel D. Immunosuppression by mesenchymal stem cells: mechanisms and clinical applications. Stem Cell Res. Ther. 2010; 1(1):2. [PubMed: 20504283]
27. Goldring MB, Otero M. Inflammation in osteoarthritis. Curr. Opin. Rheumatol. 2011; 23(5):471–478. [PubMed: 21788902]
28. Gourevitch D, Clark L, Chen P, Seitz A, Samulewicz SJ, Heber-Katz E. Matrix metalloproteinase activity correlates with blastema formation in the regenerating MRL mouse ear hole model. Dev. Dyn. 2003; 226(2):377–387. [PubMed: 12557216]
29. Granero-Molto F, Weis JA, Miga MI, Landis B, Myers TJ, O'Rear L, Longobardi L, Jansen ED, Mortlock DP, Spagnoli A. Regenerative effects of transplanted mesenchymal stem cells in fracture healing. Stem Cells. 2009; 27(8):1887–1898. [PubMed: 19544445]
30. Grayson WL, Zhao F, Bunnell B, Ma T. Hypoxia enhances proliferation and tissue formation of human mesenchymal stem cells. Biochem. Biophys. Res. Commun. 2007; 358(3):948–953. [PubMed: 17521616]
31. Gregory CA, Gunn WG, Peister A, Prockop DJ. An Alizarin red-based assay of mineralization by adherent cells in culture: comparison with cetylpyridinium chloride extraction. Anal. Biochem. 2004; 329(1):77–84. [PubMed: 15136169]
32. Guerne PA, Zuraw BL, Vaughan JH, Carson DA, Lotz M. Synovium as a source of interleukin 6 in vitro. Contribution to local and systemic manifestations of arthritis. J. Clin. Invest. 1989; 83(2): 585–592. [PubMed: 2464001]

NIH-PA Author Manuscript

NIH-PA Author Manuscript

NIH-PA Author Manuscript

33. Guilak F, Fermor B, Keefe FJ, Kraus VB, Olson SA, Pisetsky DS, Setton LA, Weinberg JB. The role of biomechanics and inflammation in cartilage injury and repair. Clin. Orthop. Relat. Res. 2004; (423):17–26. [PubMed: 15232421]
34. Guilak F, Lott KE, Awad HA, Cao Q, Hicok KC, Fermor B, Gimble JM. Clonal analysis of the differentiation potential of human adipose-derived adult stem cells. J. Cell. Physiol. 2006; 206(1): 229–237. [PubMed: 16021633]
35. Horie M, Sekiya I, Muneta T, Ichinose S, Matsumoto K, Saito H, Murakami T, Kobayashi E. Intra-articular Injected synovial stem cells differentiate into meniscal cells directly and promote meniscal regeneration without mobilization to distant organs in rat massive meniscal defect. Stem Cells. 2009; 27(4):878–887. [PubMed: 19350690]
36. Hunt DL, Campbell PH, Zambon AC, Vranizan K, Evans SM, Kuo HC, Yamaguchi KD, Omens JH, McCulloch AD. Early postmyocardial infarction survival in Murphy Roths Large mice is mediated by attenuated apoptosis and inflammation but depends on genetic background. Exp. Physiol. 2012; 97(1):102–114. [PubMed: 21967898]
37. Irie K, Uchiyama E, Iwaso H. Intraarticular inflammatory cytokines in acute anterior cruciate ligament injured knee. Knee. 2003; 10(1):93–96. [PubMed: 12649034]
38. Ivanovic Z. Hypoxia or in situ normoxia: The stem cell paradigm. J. Cell. Physiol. 2009; 219(2): 271–275. [PubMed: 19160417]
39. Iyer SS, Rojas M. Anti-inflammatory effects of mesenchymal stem cells: novel concept for future therapies. Expert Opin. Biol. Ther. 2008; 8(5):569–581. [PubMed: 18407762]
40. Kench JA, Russell DM, Fadok VA, Young SK, Worthen GS, Jones-Carson J, Henson JE, Henson PM, Nemazee D. Aberrant wound healing and TGF-beta production in the autoimmune-prone MRL/+ mouse. Clin. Immunol. 1999; 92(3):300–310. [PubMed: 10479535]
41. Kramer J, Bohrnsen F, Lindner U, Behrens P, Schlenke P, Rohwedel J. In vivo matrix-guided human mesenchymal stem cells. Cell. Mol. Life Sci. 2006; 63(5):616–626. [PubMed: 16482398]
42. Kruyt MC, De Bruijn J, Veenhof M, Oner FC, Van Blitterswijk CA, Verbout AJ, Dhert WJ. Application and limitations of chloromethylbenzamidodialkylcarbocyanine for tracing cells used in bone Tissue engineering. Tissue Eng. 2003; 9(1):105–115. [PubMed: 12625959]
43. Kurth TB, Dell'accio F, Crouch V, Augello A, Sharpe PT, De Bari C. Functional mesenchymal stem cell niches in adult mouse knee joint synovium in vivo. Arthritis Rheum. 2011; 63(5):1289–1300. [PubMed: 21538315]
44. Lawrence JT, Birmingham J, Toth AP. Emerging ideas: prevention of posttraumatic arthritis through interleukin-1 and tumor necrosis factor-alpha inhibition. Clin. Orthop. Relat. Res. 2011; 469(12):3522–3526. [PubMed: 21161742]
45. Lawrence RC, Felson DT, Helmick CG, Arnold LM, Choi H, Deyo RA, Gabriel S, Hirsch R, Hochberg MC, Hunder GG, Jordan JM, Katz JN, Kremers HM, Wolfe F. Estimates of the prevalence of arthritis and other rheumatic conditions in the United States. Part II. Arthritis Rheum. 2008; 58(1):26–35. [PubMed: 18163497]
46. Lee KB, Hui JH, Song IC, Ardany L, Lee EH. Injectable mesenchymal stem cell therapy for large cartilage defects--a porcine model. Stem Cells. 2007; 25(11):2964–2971. [PubMed: 17656639]
47. Lee SY, Miwa M, Sakai Y, Kuroda R, Oe K, Niikura T, Matsumoto T, Fujioka H, Doita M, Kurosaka M. Isolation and characterization of connective tissue progenitor cells derived from human fracture-induced hemarthrosis in vitro. J. Orthop. Res. 2008; 26(2):190–199. [PubMed: 17763429]
48. Leferovich JM, Bedelbaeva K, Samulewicz S, Zhang XM, Zwas D, Lankford EB, Heber-Katz E. Heart regeneration in adult MRL mice. Proc. Natl. Acad. Sci. USA. 2001; 98(17):9830–9835. [PubMed: 11493713]
49. Lennon DP, Caplan AI. Isolation of rat marrow-derived mesenchymal stem cells. Exp. Hematol. 2006; 34(11):1606–1607. [PubMed: 17046584]
50. Lewis JS, Hembree WC, Furman BD, Tippets L, Cattel D, Huebner JL, Little D, DeFrate LE, Kraus VB, Guilak F, Olson SA. Acute joint pathology and synovial inflammation is associated with increased intra-articular fracture severity in the mouse knee. Osteoarthritis Cartilage. 2011; 19(7):864–873. [PubMed: 21619936]

NIH-PA Author Manuscript

NIH-PA Author Manuscript

NIH-PA Author Manuscript

51. Li X, Makarov SS. An essential role of NF-kappaB in the “tumor-like” phenotype of arthritic synoviocytes. Proc. Natl. Acad. Sci. USA. 2006; 103(46):17432–17437. [PubMed: 17088540]
52. Li X, Mohan S, Gu W, Baylink DJ. Analysis of gene expression in the wound repair/regeneration process. Mamm. Genome. 2001; 12(1):52–59. [PubMed: 11178744]
53. Marsell R, Einhorn TA. The biology of fracture healing. Injury. 2011; 42(6):551–555. [PubMed: 21489527]
54. Matsumoto T, Okabe T, Ikawa T, Iida T, Yasuda H, Nakamura H, Wakitani S. Articular cartilage repair with autologous bone marrow mesenchymal cells. J. Cell. Physiol. 2010; 225(2):291–295. [PubMed: 20458744]
55. Maumus M, Guerit D, Toupet K, Jorgensen C, Noel D. Mesenchymal stem cell-based therapies in regenerative medicine: applications in rheumatology. Stem. Cell Res. Ther. 2011; 2(2):14. [PubMed: 21457518]
56. Meirelles Lda S, Nardi NB. Murine marrow-derived mesenchymal stem cell: isolation, in vitro expansion, and characterization. Br. J. Haematol. 2003; 123(4):702–711. [PubMed: 14616976]
57. Morikawa S, Mabuchi Y, Kubota Y, Nagai Y, Niibe K, Hiratsu E, Suzuki S, Miyauchi-Hara C, Nagoshi N, Sunabori T, Shimmura S, Miyawaki A, Nakagawa T, Suda T, Okano H, Matsuzaki Y. Prospective identification, isolation, and systemic transplantation of multipotent mesenchymal stem cells in murine bone marrow. J. Exp. Med. 2009; 206(11):2483–2496. [PubMed: 19841085]
58. Murphy JM, Fink DJ, Hunziker EB, Barry FP. Stem cell therapy in a caprine model of osteoarthritis. Arthritis Rheum. 2003; 48(12):3464–3474. [PubMed: 14673997]
59. Nemeth K, Leelahavanichkul A, Yuen PS, Mayer B, Parmelee A, Doi K, Robey PG, Leelahavanichkul K, Koller BH, Brown JM, Hu X, Jelinek I, Star RA, Mezey E. Bone marrow stromal cells attenuate sepsis via prostaglandin E(2)-dependent reprogramming of host macrophages to increase their interleukin-10 production. Nat. Med. 2009; 15(1):42–49. [PubMed: 19098906]
60. Ortiz LA, Dutreil M, Fattman C, Pandey AC, Torres G, Go K, Phinney DG. Interleukin 1 receptor antagonist mediates the antiinflammatory and antifibrotic effect of mesenchymal stem cells during lung injury. Proc. Natl. Acad. Sci. USA. 2007; 104(26):11002–11007. [PubMed: 17569781]
61. Peister A, Mellad JA, Larson BL, Hall BM, Gibson LF, Prockop DJ. Adult stem cells from bone marrow (MSCs) isolated from different strains of inbred mice vary in surface epitopes, rates of proliferation, and differentiation potential. Blood. 2004; 103(5):1662–1668. [PubMed: 14592819]
62. Phinney DG, Kopen G, Isaacson RL, Prockop DJ. Plastic adherent stromal cells from the bone marrow of commonly used strains of inbred mice: variations in yield, growth, and differentiation. J. Cell. Biochem. 1999; 72(4):570–585. [PubMed: 10022616]
63. Phinney DG, Prockop DJ. Concise review: mesenchymal stem/multipotent stromal cells: the state of transdifferentiation and modes of tissue repair--current views. Stem Cells. 2007; 25(11):2896–2902. [PubMed: 17901396]
64. Pickvance EA, Oegema TR Jr. Thompson RC Jr. Immunolocalization of selected cytokines and proteases in canine articular cartilage after transarticular loading. J. Orthop. Res. 1993; 11(3):313–323. [PubMed: 7686974]
65. Prockop DJ. “Stemness” does not explain the repair of many tissues by mesenchymal stem/multipotent stromal cells (MSCs). Clin. Pharmacol. Ther. 2007; 82(3):241–243. [PubMed: 17700588]
66. Prockop DJ, Oh JY. Mesenchymal stem/stromal cells (MSCs): role as guardians of inflammation. Mol. Ther. 2012; 20(1):14–20. [PubMed: 22008910]
67. Richter W. Mesenchymal stem cells and cartilage in situ regeneration. J. Intern. Med. 2009; 266(4):390–405. [PubMed: 19765182]
68. Scanzello CR, McKeon B, Swaim BH, DiCarlo E, Asomugha EU, Kanda V, Nair A, Lee DM, Richmond JC, Katz JN, Crow MK, Goldring SR. Synovial inflammation in patients undergoing arthroscopic meniscectomy: molecular characterization and relationship to symptoms. Arthritis Rheum. 2011; 63(2):391–400. [PubMed: 21279996]
69. Schulze-Tanzil G, Zreiqat H, Sabat R, Kohl B, Halder A, Muller RD, John T. Interleukin-10 and articular cartilage: experimental therapeutical approaches in cartilage disorders. Curr. Gene Ther. 2009; 9(4):306–315. [PubMed: 19534651]

NIH-PA Author Manuscript

NIH-PA Author Manuscript

NIH-PA Author Manuscript

70. Seifer DR, Furman BD, Guilak F, Olson SA, Brooks SC 3rd, Kraus VB. Novel synovial fluid recovery method allows for quantification of a marker of arthritis in mice. Osteoarthritis Cartilage. 2008; 16(12):1532–1538. [PubMed: 18538588]
71. Short BJ, Brouard N, Simmons PJ. Prospective isolation of mesenchymal stem cells from mouse compact bone. Methods Mol. Biol. 2009; 482:259–268. [PubMed: 19089361]
72. Soleimani M, Nadri S. A protocol for isolation and culture of mesenchymal stem cells from mouse bone marrow. Nat. Protoc. 2009; 4(1):102–106. [PubMed: 19131962]
73. Toghraie FS, Chenari N, Gholipour MA, Faghih Z, Torabinejad S, Dehghani S, Ghaderi A. Treatment of osteoarthritis with infrapatellar fat pad derived mesenchymal stem cells in Rabbit. Knee. 2011; 18(2):71–75. [PubMed: 20591677]
74. Tropel P, Noel D, Platet N, Legrand P, Benabid AL, Berger F. Isolation and characterisation of mesenchymal stem cells from adult mouse bone marrow. Exp. Cell Res. 2004; 295(2):395–406. [PubMed: 15093739]
75. Tsai CC, Chen YJ, Yew TL, Chen LL, Wang JY, Chiu CH, Hung SC. Hypoxia inhibits senescence and maintains mesenchymal stem cell properties through down-regulation of E2A-p21 by HIF-TWIST. Blood. 2011; 117(2):459–469. [PubMed: 20952688]
76. Ueno M, Lyons BL, Burzenski LM, Gott B, Shaffer DJ, Roopenian DC, Shultz LD. Accelerated wound healing of alkali-burned corneas in MRL mice is associated with a reduced inflammatory signature. Invest. Ophthalmol. Vis. Sci. 2005; 46(11):4097–4106. [PubMed: 16249486]
77. van der Kraan PM, Vitters EL, van Beuningen HM, van de Putte LB, van den Berg WB. Degenerative knee joint lesions in mice after a single intra-articular collagenase injection. A new model of osteoarthritis. J. Exp. Pathol. 1990; 71(1):19–31.
78. Wakitani S, Imoto K, Yamamoto T, Saito M, Murata N, Yoneda M. Human autologous culture expanded bone marrow mesenchymal cell transplantation for repair of cartilage defects in osteoarthritic knees. Osteoarthritis Cartilage. 2002; 10(3):199–206. [PubMed: 11869080]
79. Wan DC, Shi YY, Nacamuli RP, Quarto N, Lyons KM, Longaker MT. Osteogenic differentiation of mouse adipose-derived adult stromal cells requires retinoic acid and bone morphogenetic protein receptor type IB signaling. Proc. Natl. Acad. Sci. USA. 2006; 103(33):12335–12340. [PubMed: 16894153]
80. Ward BD, Furman BD, Huebner JL, Kraus VB, Guilak F, Olson SA. Absence of posttraumatic arthritis following intraarticular fracture in the MRL/MpJ mouse. Arthritis Rheum. 2008; 58(3): 744–753. [PubMed: 18311808]
81. Xu S, De Becker A, Van Camp B, Vanderkerken K, Van Riet I. An improved harvest and in vitro expansion protocol for murine bone marrow-derived mesenchymal stem cells. J. Biomed. Biotechnol. 2010; 2010:105940. [PubMed: 21197440]
82. Zachos T, Diggs A, Weisbrode S, Bartlett J, Bertone A. Mesenchymal stem cell-mediated gene delivery of bone morphogenetic protein-2 in an articular fracture model. Mol. Ther. 2007; 15(8): 1543–1550. [PubMed: 17519894]
83. Zachos TA, Bertone AL, Wassenaar PA, Weisbrode SE. Rodent models for the study of articular fracture healing. J. Invest. Surg. 2007; 20(2):87–95. [PubMed: 17454393]
84. Zhu H, Guo ZK, Jiang XX, Li H, Wang XY, Yao HY, Zhang Y, Mao N. A protocol for isolation and culture of mesenchymal stem cells from mouse compact bone. Nat. Protoc. 2010; 5(3):550–560. [PubMed: 20203670]
85. Zins SR, Amare MF, Anam K, Elster EA, Davis TA. Wound trauma mediated inflammatory signaling attenuates a tissue regenerative response in MRL/MpJ mice. J. Inflamm. 2010; 7:25.

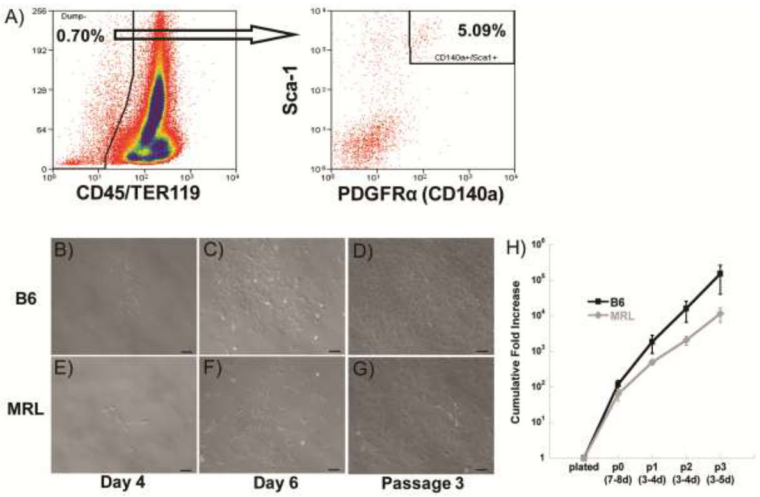

Figure 1.

Cell sorting and expansion. A) Sorting strategy for representative MRL mesenchymal stem cell (MSC) isolation, with arrow indicating only $CD45^{-}$,$TER\text{-}119^{-}$ cells are shown in the second plot. B,E) MSCs plated down after sorting; C,F) Colonies expand rapidly; D,G) Cells retain morphology and rapid growth. Scale bars = 100 μm. H) Cumulative fold increase at 2% O_2; results averaged from 3 isolations.

NIH-PA Author Manuscript
NIH-PA Author Manuscript
NIH-PA Author Manuscript

NIH-PA Author Manuscript
NIH-PA Author Manuscript
NIH-PA Author Manuscript

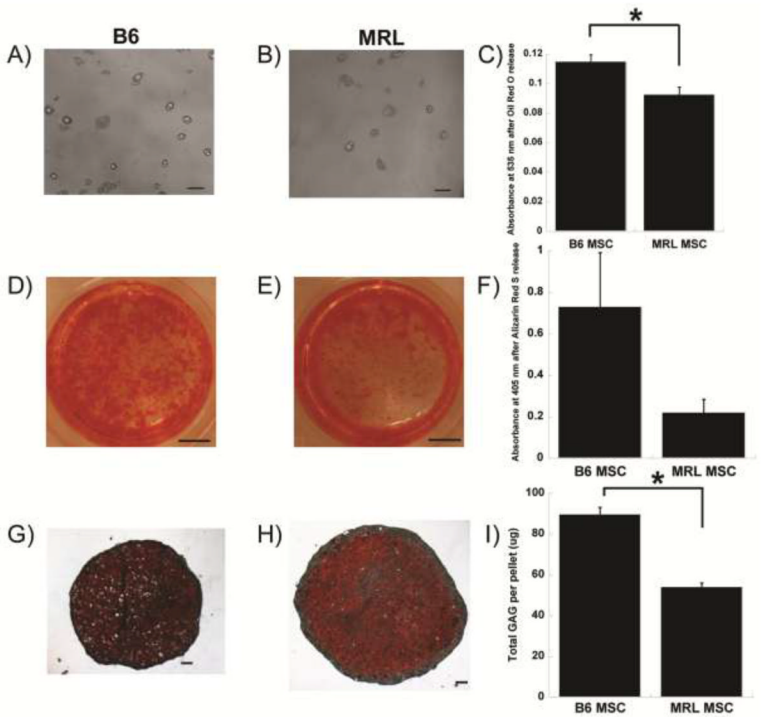

Figure 2.

Multi-lineage differentiation. A,B) Adipogenic lipid accumulation; D,E) Osteogenic Alizarin Red S staining; G,H) Chondrogenic Safranin-O/Fast Green staining. C,F,I) Quantification, results from ≥3 samples per group of one representative isolation with standard error of the mean displayed. Asterisk indicates significant effect by *t*-test. Scale bar = 100 μm (A,B,G,H) or 25 mm (D,E).

NIH-PA Author Manuscript

NIH-PA Author Manuscript

NIH-PA Author Manuscript

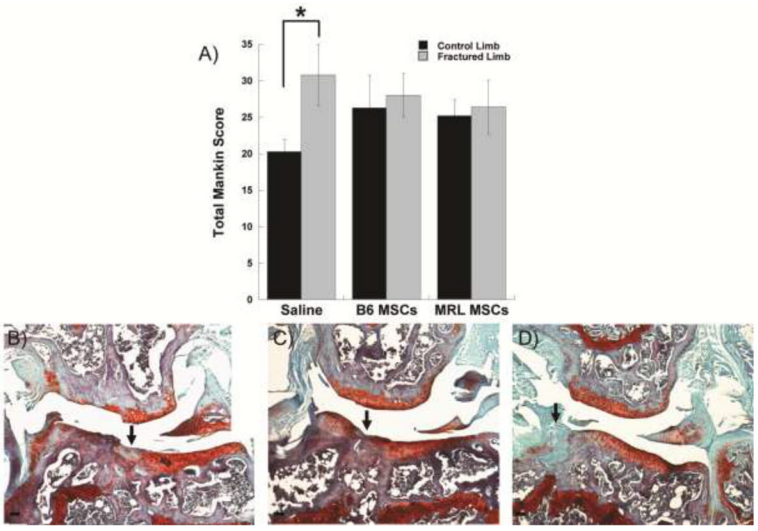

Figure 3.

Evaluation of post-traumatic arthritis. A) Total joint modified Mankin score of joint degeneration, mean of ≥7 joints per group. Asterisk indicates significant effect by ANOVA, Fisher's post-hoc. B–D) Safranin-O/Fast-Green/Hematoxylin stained coronal section showing the articulation of the lateral femur (top) and lateral tibia (bottom) 8 weeks after fracture. Joint of each group with the highest structural Mankin scores on lateral side shown. Scale bar = 100 μm, arrow indicates fracture site.

NIH-PA Author Manuscript
NIH-PA Author Manuscript
NIH-PA Author Manuscript

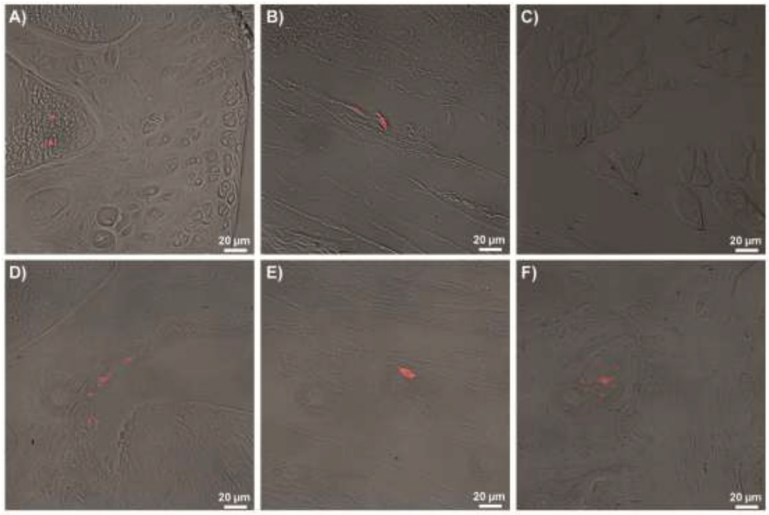

Figure 4.
Cell tracking. CM-DiI labeling of stem cells before injection. B6 MSCs were found at day 1 in A) bone marrow, B) synovium, and C) muscle. B6 MSCs were also found at D) day 3 in the lateral femoral synovium, E) day 7 near lateral ligamentous tissue, and F) 8 weeks in the tibial subchondral bone.

NIH-PA Author Manuscript

NIH-PA Author Manuscript

NIH-PA Author Manuscript

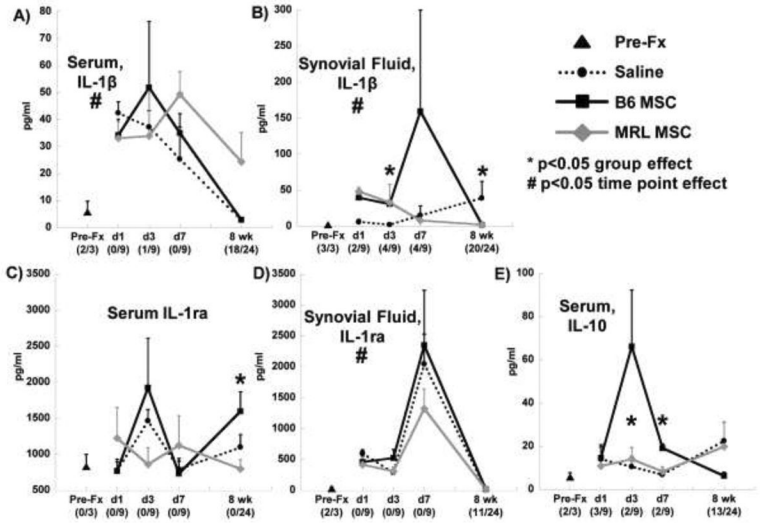

Figure 5.

Systemic (serum) and local (synovial fluid from fractured knee) cytokine concentrations. A,B) Interleukin 1β (IL-1β); C–D) Interleukin 1 receptor antagonist (IL-1ra); E) Interleukin 10 (IL-10). Number of undetectable samples in parentheses. Asterisk indicates significant effect of treatment group at that time point by Kruskal-Wallis Test. Pre-fracture (Pre-Fx) and days 1, 3, 7 (n=3), and 8 weeks (n=8) after fracture.

NIH-PA Author Manuscript
NIH-PA Author Manuscript
NIH-PA Author Manuscript

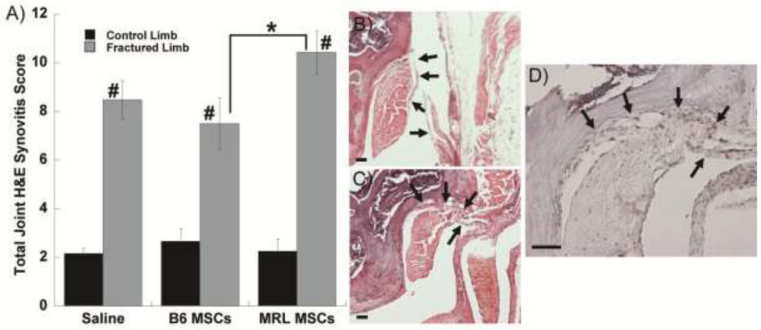

Figure 6.

Synovial response to fracture. A) Total joint synovitis score, mean of ≥7 joints per group. Significance to group shown (*) or all control groups (#) by ANOVA, Fisher's post-hoc. B) Hematoxylin/Eosin staining of lateral femur from a non-fractured control limb without synovial inflammation (mirror image shown). C) Hematoxylin/Eosin staining of lateral femur 8 weeks after fracture and injection of B6 MSCs. D) F4/80 staining for macrophages in the same joint as panel C. In all panels scale bar = 50 μm and arrows indicate synovium.

NIH-PA Author Manuscript
NIH-PA Author Manuscript
NIH-PA Author Manuscript

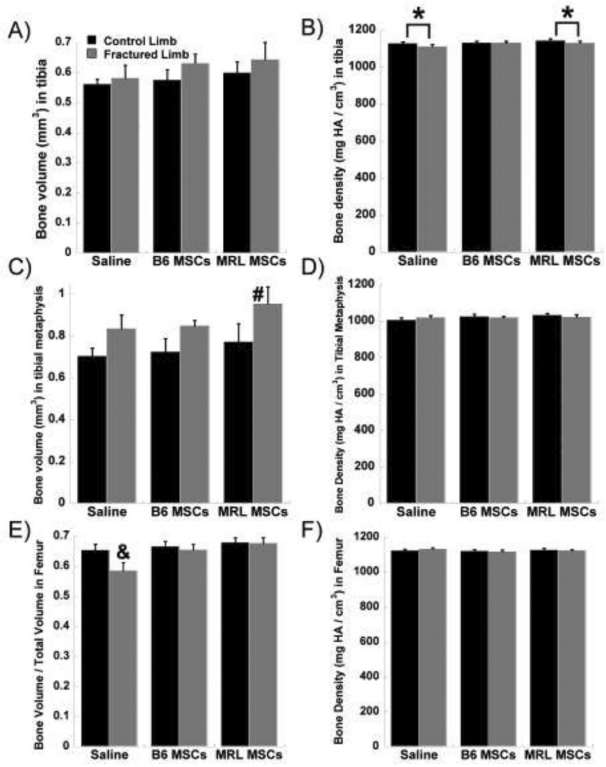

Figure 7.

Morphological bone changes. A) Tibial bone volume; B) Tibial bone density; C) Bone volume in tibial metaphysis; D) Bone density in tibial metaphysis; E) Femoral bone volume / total volume; F) Femoral bone density. Significance to contralateral control (*), all control groups (#), or all groups (&) by ANOVA, Fisher's post-hoc; 8 joints per group.